

TECHNOLOGY DEVELOPMENTS TOWARDS A COMBINED XRD-XRF INSTRUMENT FOR PLANETARY SURFACE ANALYSIS

N. Nelms¹, A. Holland², D. Talboys¹, I. Hutchinson², D. Simpson², G. Cressey³, P. Bland⁴

¹Space Research Centre, University of Leicester, Leicester, LE1 7RH, UK, nin@star.le.ac.uk.

²e2v centre for electronic imaging, Brunel University, Uxbridge, UB8 3PH, UK.

³Dept. Mineralogy, The Natural History Museum, Cromwell Road, London, SW7 5BD, UK.

⁴Dept. Earth Science & Engineering, Royal School of Mines, Imperial College, London, SW7 2AZ, UK.

ABSTRACT

Geochemical analysis of the surface material of terrestrial type planets is of fundamental importance in understanding the geological context of the planetary environment. Consequently this analysis should be performed whenever possible and indeed this has occurred on a number of previous landers. Current techniques include X-ray fluorescence (XRF) and Rutherford back-scattering of alpha particles, which provide information on the elemental composition of the sample. However, geological understanding can be greatly improved if the mineral structure of the sample can also be determined. The dominant method used for mineralogical identification of geological samples in earth-based laboratories is X-ray diffraction (XRD), which analyses the crystal lattice structure to decipher the constituent minerals. When XRD is combined with XRF it creates a powerful tool for characterisation of the geochemical, mineralogical and, by inference, the petrological nature of geologic material. To date no XRD instrument has been operated on the surface of another planet but a number of combined XRD – XRF instruments for planetary surface operation are currently under development in the US, Europe and Japan. In this paper we describe a number of technology developments that are taking place in the UK aimed at developing an efficient excitation and detection system for such a combined XRD-XRF instrument.

1. INTRODUCTION

A combined X-ray diffraction/X-ray fluorescence instrument deployed on a planetary lander or rover is able to characterise the mineralogical and geochemical makeup of local geological materials. Taken together these measurements can provide unambiguous mineral identification which can help determine the past conditions and context under which those samples were formed and so make an important contribution to interpreting the nature, origin and evolution of the geological environment. Such an instrument has never been deployed on another planetary surface but is currently baselined by both

NASA for the Mars Science laboratory (Chemin) [1] and by ESA for the ExoMars rover [2]. In the case of Mars, the surface geochemistry has been measured by instruments on the two Viking landers, Mars Pathfinder's Sojourner Rover and the two Mars Exploration Rovers. The Viking landers made the first analyses of the Martian regolith [3]. The Pathfinder Sojourner rover was first to analyse rocks on Mars [4] while the two Mars Exploration Rovers detected chemical signatures in rocks that indicate alteration by water [5,6]. However, the use of this geochemical data to infer rock mineralogy (and hence petrology) involves some uncertainty since different mineral assemblages may have the same composition. In contrast, the X-ray diffraction technique probes the crystal structure of minerals and is able to make a direct measurement of mineralogy.

An XRD/XRF instrument deployed on a Mars rover can perform several science investigations but of considerable contemporary interest is the search for evidence of life. This consists of investigating the mineralogy of lithologies that may harbour fossilized life or extant life [7]. The instrument can also search for evidence that liquid water influenced the evolution of the landing site [8] which has important implications for the past or present biological habitability of the landing area [9]. Mineral deposits formed in the presence of liquid water detected from orbit, by TES [10] and OMEGA [11], can be investigated *in situ*. Ground truth measurements have a valuable role in constraining the interpretation of remote sensing data since it can provide definitive characterisation of the mineralogy of individual rocks.

A practical XRD instrument comprises three main elements – an X-ray source, a prepared sample and a detector. These can be arranged in a number of different ways around two main modes of operation – transmission or reflection (see figure 1). In transmission mode X-rays are diffracted (and fluoresced) by a prepared sample in the path of the incident X-ray beam while in reflection mode both the source and the detector are located on the same side of the sample. Each geometry has advantages and disadvantages based mostly on sample

presentation but both arrangements require a powdered sample that is well prepared in terms of consistent grain size. Current work described in this paper is concentrating for the most part on reflection geometry due to sample sharing with other instruments.

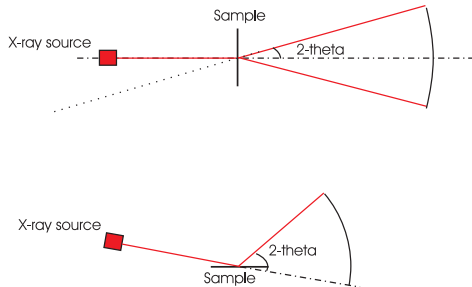


Figure 1. Transmission (top) and reflection (bottom) diffraction geometries showing sample orientation and 2-theta angle.

2. X-RAY SOURCE

XRD requires a coherent X-ray source that is both monochromatic and has low beam divergence. Preliminary studies have indicated little benefit from the use of X-ray optics for this application, and so beam collimation is more readily achieved using a simple pinhole placed at a suitable distance from the source. In our developments we are concentrating our efforts into the use of X-ray tubes rather than, for example, an ^{55}Fe radioactive source since it is possible to achieve much higher X-ray flux from the tube source. Initial trials using a standard Kevex X-ray tube with Cu anode have resulted in a flux of approximately $20,000 \text{ s}^{-1}$ through an $80 \mu\text{m}$ hole in a tungsten foil (see figure 2) placed at a distance of 10 cm from the focal spot.

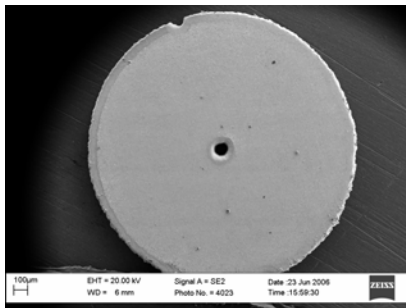


Figure 2. $80\mu\text{m}$ pin-hole in tungsten foil used for X-ray beam collimation.

Given the $\sim 250 \mu\text{m}$ diameter of X-ray spot in the tube, this equates to a beam divergence of

approximately 0.07° which is suitable for our requirements. We are initially conducting further trials using an Oxford Instruments Eclipse III portable X-ray tube [12], and later hope to use the planned micro-focus version with a target spot size of $50 \mu\text{m}$. Using this tube, suitable collimation for a 0.1° beam divergence could be obtained using an $80\mu\text{m}$ pinhole placed at a distance of 50mm. This would result in significantly more flux (or lower power) than the flux measured to-date. The use of such an X-ray tube would need to pass qualification testing, particularly to survive the entry descent and landing, and the operating temperature. Diffraction is an inherently inefficient process (typically 10^{-4} or 10^{-5}) and even with a high incident flux detected count-rates can be very low.

3. DETECTORS

Solid-state semiconductor detectors for X-ray detection are available in a number of different formats, both single pixel and as 1D and 2D arrays. High-resolution laboratory X-ray diffractometers tend to use a silicon diode detector on a movable arm to measure the diffraction distribution. Mechanisms of any sort are not preferred for spacecraft operations due to inherent reliability problems. Consequently a position-sensitive detector (either 1D or 2D) provides a convenient method for detecting the diffraction pattern without movement – see figure 3.

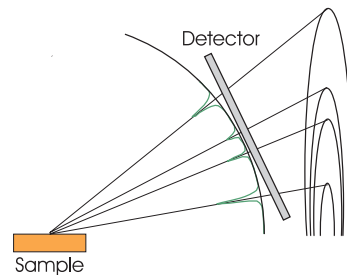


Figure 3. Diffraction measurement using position sensitive detector.

Charge coupled device (CCD) detectors have a long heritage in space operation as X-ray detectors [13]. With direct X-ray detection (in the $0.5 - 10 \text{ keV}$ range), low noise operation and good spatial resolution (pixel size of order $10 - 40 \mu\text{m}$) CCDs can make excellent detectors for XRD. When operated in photon-counting mode the energy of each X-ray can be determined allowing discrimination between fluoresced and diffracted photons. This enables simultaneous construction of an XRF histogram and an XRD diffractogram (figure 4), providing

information on both the elemental composition and the mineralogical structure.

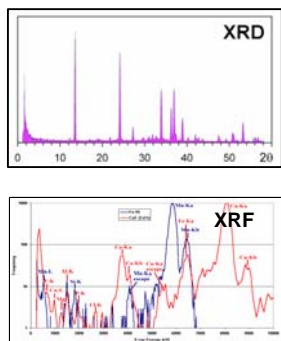


Fig. 4. Sample XRD 2θ diffractogram plot and XRF histogram.

Detector parameters have a large impact on the overall performance of an XRD instrument especially when a position-sensitive array is used. In terms of the diffraction pattern the choice of detector affects the area of the diffraction rings sampled and the angular resolution of the resultant diffraction pattern. Sampling the diffraction pattern with a 1D (linear) array or narrow 2D array minimises the raw data (due to the small number of pixels) and can provide high resolution. However, with predicted very low X-ray flux rates (see section 2) collecting area most probably needs to be maximised. This can be achieved by using a wider 2D array but for practical reasons of instrument volume, power and mass means that a lower angular resolution has to be accepted. As part of this development programme two different custom CCD designs are being produced by e2v technologies Ltd [14]. They are both frame-transfer CCDs, which allows effectively zero dead-time during operation and have small pixels ($13.5 \mu\text{m}$ square). The frame-transfer region of both devices has a reduced area (25% instead of 50%) to maximise the collecting area of the CCD. The two devices are identical except for number of pixels (and hence area) – the two formats are shown in figure 5.

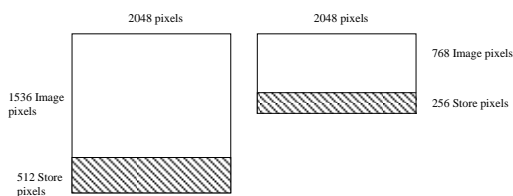


Fig. 5. Proposed CCD formats for development programme.

The devices are being manufactured using deep-depletion silicon in order to provide good X-ray

quantum efficiency. They are front-illuminated and have inverted mode operation for reduced dark-current at non-cryogenic temperatures.

As discussed above the format of the detector affects the performance of the instrument. This argument can be extended to include the use of multiple detectors arranged in array. It is planned to study a number of different array geometries based on the two CCD structures shown in figure 5. The proposed arrangements are shown in figure 6.

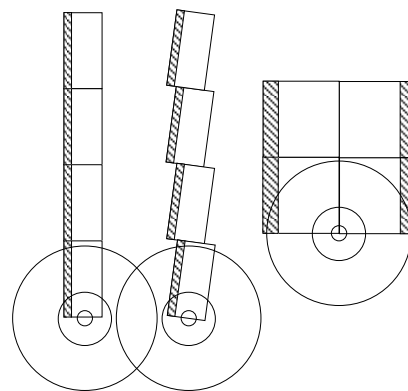


Figure 6. Proposed CCD detector array geometries. The interaction with (part of) the diffraction rings is shown.

The first two linear arrangements provide high angular resolution ($\sim 0.05^\circ$ over a 60° range) coverage but with a narrow collecting area. The offset linear arrangement removes dead space between the detectors but further complicates diffraction pattern correction. The third 2×2 array presents the best collecting area but suffers from reduced angular resolution ($\sim 0.15^\circ$ over a 60° range).

As stated above, low noise operation is necessary for X-ray photon counting and a prerequisite for this is to cool the CCD in order to reduce leakage (dark) current generation. Operating temperatures of order 173 - 243 K are typically required. At the higher end of this range more precise thermal control is required to prevent significant fluctuations in dark current levels. Typical total noise requirements are discussed in section 4.1.3. Read-out rates are driven by a number of factors including dark current generation, read-noise requirements and power consumption. With reasonable cooling ($< 243 \text{ K}$) exposure times of order a few seconds can be tolerated with regard to dark current. On-chip binning can also be applied to reduce the number pixels that need to be read, in this case driven by angular resolution requirements and curvature of the diffraction pattern. For the CCDs being developed numbers of (binned) pixels to read are either 250,000 or 500,000. Read-out rates of 100

– 200 kpixels/second will meet the few second exposure time limit.

4. ELECTRONICS

Although CCDs are ideally suited to a combined XRD-XRF instrument they are not simple devices to operate. They require a range of bias voltages and a number of different clocks. For low noise operation, required for both XRD and XRF, the output signal from the CCD also needs to be processed. Figure 7 is a block diagram of a CCD detector array showing the typical drive signals for both the detector and the signal processing electronics.

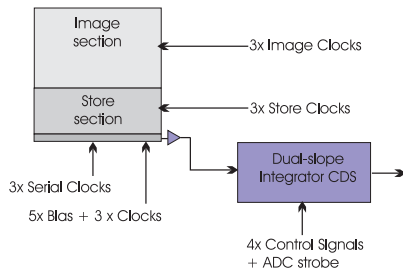


Fig. 7. Typical CCD control signals.

4.1 Bias Voltage Generation

e2v CCDs typically require bias voltages in the range of 0 to 35 V. Maximum current requirement is for the output drain of the on-chip amplifier, typically 2 – 5 mA (at 28 – 32 V). These can be easily generated using an operational amplifier buffer coupled with a low-pass filter to reduce noise injection. Once optimised for a particular CCD, the bias voltages do not usually need to be altered and can be fixed in the design.

4.1.2 Clock Waveform Generation

A number of approaches are possible for producing the clock waveforms that are required. For an application such as this, the clock pattern is essentially fixed with possible variable parameters for image integration time and on-chip binning. We are adopting an FPGA approach since space-qualified devices are readily available. The CCDs being used are of frame-transfer design which provides essentially zero dead-time during read-out. Consequently extra clocks are required to control the storage section of the detector. The clocking outputs from the FPGA are TTL level and need to be level shifted for correct CCD operation. Typical maximum clock levels for e2v devices are of order 15 V, with a 0 V minimum. Proprietary level shifters (clock drivers), with high current output, are available from

Intersil (Elantec) although qualification for operation in a space environment needs to be verified. Bias generation is also required for the high-level of the clock driver, appropriately decoupled in order to provide the peak current requirements of the various clock loads.

4.1.3 CCD Signal Processing

The noise performance of the CCD depends upon a number of things, not least dark-current generation which is temperature dependent, and output read-noise. CCD noise performance is usually quoted as an equivalent noise charge (enc) in electrons rms. An enc < 10 electrons rms is typically needed in order to perform XRF with < 30 electrons for XRD. When the CCD is cooled and/or operated fast enough the read-noise is dominated by the CCD output node reset noise, i.e. the dc level of the CCD output amplifier is reset after each pixel charge is read and the uncertainty in this reset level is of order 100s electrons rms.

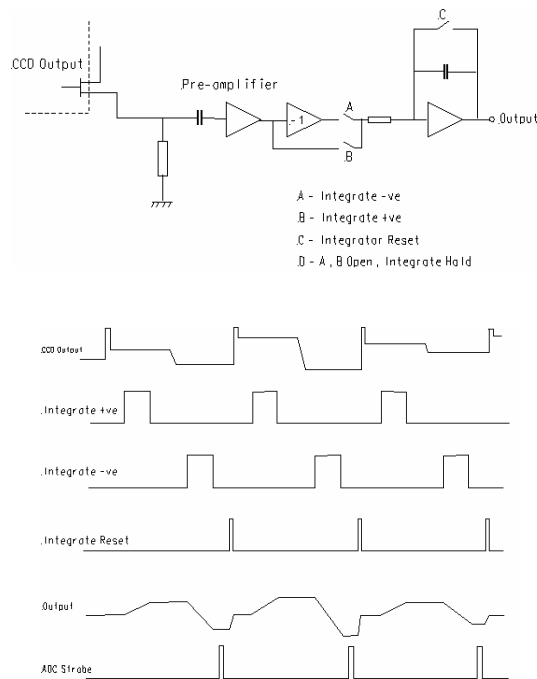


Fig. 8. CCD signal processing – dual-slope integrator technique. Top – typical dual-slope integrator schematic, bottom – associated control and output waveforms. The actual circuit also includes an input clamp to avoid saturation from reset feed-through.

Left like this the CCD would be incapable of X-ray photon energy analysis and construction of XRD diffractograms and XRF histograms would be impossible. The reset noise is removed using correlated double sampling (CDS). A number of

different schemes exist but they all perform the same function. The output amplifier of the CCD is reset and the reset level is sampled. The pixel charge is then clocked onto the output node and the output sampled again. These two samples are then differenced (or correlated) and the result is the pixel charge level independent of the uncertain reset level. As mentioned above a number of different schemes for CDS processing exist and we have chosen a dual-slope integration technique – see figure 8. This is not the fastest scheme but high-speed read-out is not required (see section 3) and the technique benefits from improved noise reduction provided by the integration technique. A single channel version of the dual-slope integrator CDS has been built and tested with noise performance of 5 electrons rms (over-scan) at 100 kHz when operating with an e2v CCD42 – see figure 9.

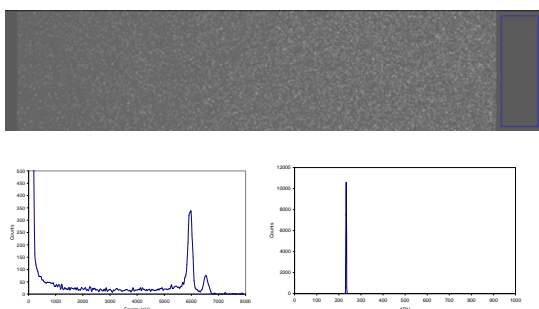


Fig. 9. Prototype dual-slope integrator performance. Top - CCD image with X-rays from ^{55}Fe source at 5.9 keV and 6.4 keV showing over-scan region at the right. Bottom left – X-ray histogram, FWHM at 5.9 keV is 200 eV. Bottom right – over-scan noise histogram, enc is 5 electrons rms. X-ray performance is limited by dark-current from CCD at $-50\text{ }^\circ\text{C}$. 100 kHz pixel read-out rate with $2.8\text{ }\mu\text{s}$ integrator time.

For the flight-type CDS design we are developing a dual-channel hybrid circuit. One or two of these devices will be used depending upon the size of the detector array, either 2 or 4 CCDs. The hybrid circuit approach has a number of advantages over an ASIC design. The hybrid is cheaper for small quantities, it can be built around radiation-hard and/or space qualified devices and performance is easier to verify at the prototype stage. The hybrid is also usually housed in sealed metal package which contributes further to the environmental durability. Our design is based on Analog Devices OP42 amplifiers and ADG201HS analogue switches, both of which have radiation and environmental test data available. Both devices are of course available as dice. At the time of writing the hybrid design is complete and has been sent out for manufacture.

4.1.4 CCD Data Processing – Hardware

With an array of 4 CCD detectors operating in photon counting mode raw data rates can be high. In order to shield the uplink from excessive data quantities on-board processing can be performed. To this end we have included a digital signal processor (DSP) between the analogue to digital converters and the output bus (the laboratory prototype uses a USB output bus to facilitate PC interfacing).

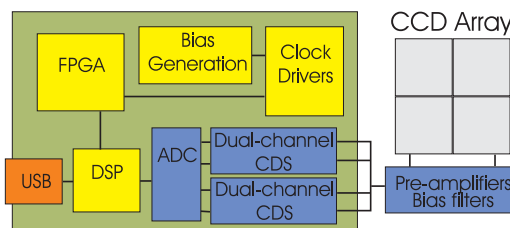


Fig. 10. Overall block diagram of proposed flight-type CCD array drive electronics. The USB interface is to facilitate laboratory testing.

As indicated in section 4.1.3 the CDS hybrid is already in manufacture. The design for the CCD drive electronics is underway (figure 10) and we aim to have a working prototype of the whole system by the end of 2006.

5. DATA PROCESSING

The reduction of data volumes (and consequently rates) requires some on-board processing and since event rates are low this can be performed in real-time. This is achieved using a dedicated DSP that will take digitised CCD data as an input and produce XRD diffractograms and XRF histograms as output.

The DSP will have a number of functions related to data processing including:

- Dynamic calibration – this is possible using the diffracted photons of known energy.
- Event reconstruction. X-ray photons that deposit their charge into more than one pixel can be ‘reconstructed’ to recover the original energy. These can then contribute to XRF and XRD histograms.
- Diffracted/fluoresced photon discrimination based on photon energy.
- Background rejection.
- Construction of XRF energy histogram.
- Diffraction pattern curvature correction.
- Construction of $K\alpha$ and $K\beta$ 2θ XRD diffractograms.

The DSP will also be responsible for CCD clock sequencer parameter setting since it provides the only interface to the outside world. A 'raw-data' mode will also be included for diagnostic purposes to allow direct visualisation of CCD images.

6. CONCLUSIONS

A combined XRD-XRF instrument that is able to perform *in situ* analyses on surface samples of another planet can provide the geochemical and mineralogical information with which to contextualise the local environment. It is also capable of providing valuable ground truth measurements for the current and future generations of orbital instruments. The technology developments described in this paper are aimed at enabling such an instrument to be produced initially for Mars but possibly also for the Moon and other terrestrial type surfaces.

7. REFERENCES

1. Blake, D.F., Sarrazin, P., Bish, D.L., Feldman, S., Chipera, S.J., Vaniman, D.T., Collins, S.A. "Definitive Mineralogical Analysis of Mars Analogs Using the CheMin XRD/XRF Instrument", Lunar and Planetary Science Conf XXXV, 2004.
2. <http://www.esa.int/esaMI/Aurora>
3. Clark, B. C., A. K. Baird, R. J. Weldon, D. M. Tsusaki, L. Schnabel, M. P. Candelaria, "Chemical composition of Martian fines", J. Geophys. Res, 87, 10059-10067, 1982.
4. Rieder, R., T. Economou, H. Wänke, A. Turkevich, J. Crisp, J. Brückner, G. Dreibus, H. Y. McSween Jr., "The chemical composition of martian soil and rocks returned by the mobile Alpha Proton X-ray Spectrometer: Preliminary results from the X-ray mode", Science, 278, no. 5344, 1771-1774, 1997.
5. Rieder, R., R. Gellert, R. C. Anderson, J. Brückner, B. C. Clark, G. Dreibus, T. Economou, G. Klingelhöfer, G. W. Lugmair, D. W. Ming, S. W. Squyres, C. d'Uston, H. Wänke, A. Yen, J. Zipfel, "Chemistry of rocks and soils at Meridiani Planum from the Alpha Particle X-ray Spectrometer", Science, 306/5702, 1746-1749, 2004.
6. Gellert, R., R. Rieder, J. Brückner, B. Clark, G. Dreibus, G. Klingelhofer; G. Lugmair, D. Ming, D. H. Wänke, A. Yen, J. Zipfel, S. Squyres, "The Alpha Particle X-Ray Spectrometer (APXS): Results from Gusev Crater and calibration report", J. Geophys. Res, 111/E2, 2555, 2006.
7. Vaniman, D., D. Bish, D. Blake, S. T. Elliot, P. Sarrazin, S. A. Collins, S. Chipera, "Landed XRRF/XRD analysis of prime targets in the search for past or present Martian life", J. Geophys. Res, 103/E13, 31477-31489, 1998.
8. Blake, D. F., P. Sarrazin, S. J. Chipera, D. L. Bish, D. T. Vaniman, Y. Bar-Cohen, S. Sherrit, S. Collins, B. Boyer, C. Bryson, J. King, "Definitive mineralogical analysis of Martian rocks and soil using the CheMin XRD/XRF instrument and the USDC sampler", Sixth international conference on Mars, 2003.
9. Harland, D. M., "Water and the Search for Life on Mars", Springer-Verlag, 2005.
10. Christensen, P.R., Bandfield, J.L., Clark, R.N., Edgett, K.S., Hamilton, V.E., Hoefen, T., Kieffer, H. H., Kuzmin, R. O. , Lane, M. D., Malin, M.C., Morris, R.V., Pearl, J.C., Pearson, R., Roush, T.L. , Ruff, S.W. , Smith, M.D., "Detection of crystalline hematite mineralization on Mars by the Thermal Emission Spectrometer: Evidence for near-surface water", J. Geophys. Res, 105/E4, 9623-9643, 2000.
11. Bibring, J.-P., Langevin, Y., Gendrin, A., Gondet, B., Poulet, F., Berthe, M., Soufflot, A., Arvidson, R., Mangold, N., Mustard, J., Drossart, P. and the OMEGA team, "Mars Surface Diversity as Revealed by the OMEGA/ Mars Express Observations", Science, 307, 1576-1581, 2005.
12. www.oxfordxtg.com
13. Holland, A.D., "X-ray spectroscopy using MOS CCDs", Nucl. Instr. Meth. A, 377, 334-339, 1996.
14. www.e2v.com